



Wetenhall, B. and Race, J.M. and Aghajani, H. and Barnett, J. (2017) The main factors affecting heat transfer along dense phase CO₂ pipelines. *International Journal of Greenhouse Gas Control*, 63. 86–94. ISSN 1750-5836 , <http://dx.doi.org/10.1016/j.ijggc.2017.05.003>

This version is available at <https://strathprints.strath.ac.uk/60678/>

Strathprints is designed to allow users to access the research output of the University of Strathclyde. Unless otherwise explicitly stated on the manuscript, Copyright © and Moral Rights for the papers on this site are retained by the individual authors and/or other copyright owners. Please check the manuscript for details of any other licences that may have been applied. You may not engage in further distribution of the material for any profitmaking activities or any commercial gain. You may freely distribute both the url (<https://strathprints.strath.ac.uk/>) and the content of this paper for research or private study, educational, or not-for-profit purposes without prior permission or charge.

Any correspondence concerning this service should be sent to the Strathprints administrator: strathprints@strath.ac.uk

The Main Factors Affecting Heat Transfer Along Dense Phase CO₂ Pipelines

B. Wetenhall^{1*}, J.M. Race², H. Aghajani¹ and J. Barnett³

¹ School of Marine Science and Technology, Newcastle University, Newcastle, NE17RU, UK

² Department of Naval Architecture, Ocean and Marine Engineering, University of Strathclyde,
Glasgow, G4 0LZ, UK

³ National Grid, 35 Homer Road, Solihull, West Midlands, B91 3QJ, UK

ABSTRACT

Carbon Capture and Storage (CCS) schemes will necessarily involve the transportation of large volumes of carbon dioxide (CO₂) from the capture source of the CO₂ to the storage or utilisation site. It is likely that the majority of the onshore transportation of CO₂ will be through buried pipelines. Although onshore CO₂ pipelines have been operational in the United States of America for over 40 years, the design of CO₂ pipelines for CCS systems still presents some challenges when compared with the design of natural gas pipelines. The aim of this paper is to investigate the phenomenon of heat transfer from a buried CO₂ pipeline to the surrounding soil and to identify the key parameters that influence the resultant soil temperature. It is demonstrated that, unlike natural gas pipelines, the CO₂ in the pipeline retains its heat for longer distances resulting in the potential to increase the ambient soil temperature and influence environmental factors such as crop germination and water content. The parameters that have the greatest effect on heat transfer are shown to be the inlet temperature and flow rate, *i.e.* pipeline design parameters which can be dictated by the capture plant and pipeline's design and operation rather than environmental parameters. Consequently, by carefully controlling the design parameters of the pipeline it is possible to control the heat transfer to the soil and the temperature drop along the pipeline.

KEYWORDS

CO₂ pipelines, temperature profile, sensitivity analysis, heat transfer, soil temperature, hydraulic modelling, CCS



The Don Valley Power Project is co-financed by the European Union's European Energy Programme for Recovery
The sole responsibility of this publication lies with the author.
The European Union is not responsible for any use that may be made of the information contained therein.

1. INTRODUCTION

Carbon Capture and Storage (CCS) is one method of reducing carbon dioxide (CO₂) emissions into the atmosphere which would otherwise contribute towards global climate change. CCS involves capturing CO₂ from a large industrial point source (such as a power station) and transporting the CO₂ for either usage (for example for Enhanced Oil Recovery (EOR)) or for permanent storage in a

* Corresponding author: Tel: (0044) 191 2085532 ; E-mail: ben.wetenhall@ncl.ac.uk

35 geological site. Depending on the distance and availability of a suitable storage site, the transportation
36 of the CO₂ to the storage site is by means of a pipeline network, by ship based transportation or a
37 combination of both.

38

39 For the onshore pipeline transportation of CO₂, after compression at the capture plant, the CO₂
40 streams will typically be at temperatures between 30°C to 50°C and pressures between 10MPa to 20
41 MPa (Farris, 1983; Race et al., 2012) putting the CO₂ streams in either supercritical or dense phase.
42 For CO₂ pipelines, it is important to understand how the temperature of the fluid varies along the
43 pipeline, as the temperature determines the phase of the fluid and affects density, pressure drop
44 (Dongjie et al., 2012) and economics (Teh et al., 2015; Zhang et al., 2006). Colder ground conditions
45 provide greater cooling of the CO₂ stream and, as a result, lower inlet pressures are required to keep
46 the CO₂ in a liquid phase. In addition, higher densities are maintained at lower temperatures, which is
47 more efficient for pipeline transportation and better for pump operation.

48

49 When the fluid temperature is higher than that of the surrounding soil, due to the temperature
50 difference between the CO₂ and surroundings and elevation changes along the pipeline route, there
51 will be heat exchange between the CO₂ stream and the surrounding environment with the temperature
52 of the fluid getting closer to (but not necessarily reaching) ambient temperature along the length of the
53 pipeline. The heat transfer between the fluid and the surrounding soil takes place in 4 stages: firstly
54 there is forced convection from the film of fluid coating the inner surface of the pipeline, the second
55 stage of heat transfer is conduction through the pipe wall, heat transfer then proceeds via conduction
56 from the outer surface of the pipeline and through the surrounding soil. Finally there is natural
57 convection from the surface of the soil to the surrounding air. In the conduction stages through the
58 pipeline and from the pipeline to the soil, it is possible to include the effects of any pipeline coatings
59 (which may be included on the pipe internal surface, for example to, facilitate flow) and insulation on
60 the outside of the pipe. In this work coatings are neglected due to a lack of publically available
61 information on their heat transfer properties and no insulation is added to the pipeline following the
62 planned demonstration projects in the UK (Capture Power, 2016).

63

64 In natural gas pipelines the fluid generally reaches ambient temperature very rapidly but in CO₂
65 pipelines this process can be much slower. Heat transfer from the fluid to the surroundings can cause
66 environmental issues. For example, pipelines carrying warm fluid can cause heating of the
67 surrounding soil, which may result in premature crop growth and affect soil moisture and the
68 temperature along the pipeline Right of Way (ROW) (Dunn et al., 2008; Naeth et al., 1993; Neilsen et
69 al., 1990) in some circumstances. In order for a pipeline operator to be able to manage these effects, it
70 is important to understand the degree of influence that operational and environmental factors have on
71 heat flux from the fluid to the surrounding soil. Factors influencing the degree of heat flux from a

72 buried pipeline include the fluid pressure and temperature, the soil temperature, the soil type and
73 moisture content (Becker et al., 1992), the thermal conductivity of the pipeline steel and the elevation
74 profile along the pipeline route (Teh et al., 2015). Some parameters such as the temperature of the
75 fluid, operating pressure and initial temperature of the CO₂ can be controlled at the capture plant.
76 Other parameters, such as the soil type and ambient temperature are out of the control of the pipeline
77 operator.

78

79 **1.1. Heat transfer from CO₂ pipelines**

80 There is very little publically available work on heat transfer from CO₂ pipelines. The heat transfer
81 characteristics of CO₂ pipelines surrounded by water were analysed experimentally and
82 computationally by Drescher et al. (2013). They found that the water temperature has a high impact
83 on the amount of heat transfer and a range of values for the overall heat transfer coefficient for a CO₂
84 pipelines surrounded by water, finding a mean value of 44.7W/m²K. The importance to CO₂ pipeline
85 operation of the soil temperature and type, thermal conductivity of the pipeline and topography of the
86 pipeline route was highlighted in Dongjie et al. (2012) and Teh et al. (2015). They found that
87 transporting and storing liquid CO₂ can be cheaper than supercritical CO₂, that cooler ground
88 conditions can lead to cost savings and highlighted the need for further work to explore the effect of
89 burial depth and of soil thermal conductivity. The effect of pipeline operating temperature on UK
90 soils was investigated in Lake et al. (2016) who provided the first set of empirical data on soil
91 temperature and moisture profiles for CCS pipelines. There is still need for further work on how best
92 to operate a CO₂ pipeline with regards to heat transfer and experimental work into heat transfer from
93 full scale CO₂ pipelines. This work is a step towards the former.

94

95 Through pipeline simulations and a sensitivity analysis this study identifies the dominant parameters
96 affecting heat transfer from liquid CO₂ pipelines and discusses how an operator can control heat
97 transfer out of the pipeline to minimise the impact of heat transfer. Firstly a preliminary study was
98 conducted consisting of a series of eight steady-state pipeline simulations. This allowed an
99 investigation of the influence of ground temperature, flow rate, inlet temperature, burial depth, soil
100 conductivity, inlet pressure and CO₂ composition on the rate of temperature loss along the pipeline
101 and a comparison to previous results. A sensitivity analysis, using a Gaussian emulator, was then
102 performed to identify which of the parameters investigated in the preliminary analysis had the
103 strongest influence on the temperature drop along the pipeline. The Gaussian emulation approach is
104 highly computationally efficient (far fewer model runs are required compared with, for example,
105 Monte-Carlo based methods), it allows for a complete range of sensitivity measures to be computed
106 from one set of pipeline simulation results and statistical performance is included in the process. It is
107 applicable to the current study because the data from the pipeline simulations is smooth (*i.e.* there are

108 no sudden jumps when moving between data points). Smoothness was ensured by keeping the
109 pipeline simulations in the dense or supercritical phase.

110

111 **2. HYDRAULIC MODELLING OF THE CO₂ PIPELINES**

112 **2.1. Model setup**

113 The modelling approach that was adopted for this study is described in detail in (Wetenhall et al.,
114 2014). Heat transfer modelling details are given in Section 2.2 while the other details are presented in
115 summary. PIPESIM, a steady-state flow simulator (Schlumberger, 2010), was used to conduct the
116 hydraulic modelling of the CO₂ pipeline. As implemented in the software package MultiFlash
117 (Infochem, 2011), the fluid physical (density, enthalpy, compressibility and heat capacity) and phase
118 properties were determined using the Peng-Robinson Equation of State (Peng and Robinson, 1976),
119 fluid viscosity was calculated using the Pedersen model (Pedersen et al., 1984) and SUPERTRAPP
120 (NIST, 2007) was used to determine fluid thermal conductivity. Figure 1 shows a flow diagram for
121 the pipeline simulation procedure as implemented in PIPESIM. The procedure requires the
122 simultaneous solution of the conservation of mass, momentum and energy equations. From the
123 solution of these equations, the pressure and temperature drops along the length of the pipeline can be
124 calculated given two of the parameters of initial pressure, final pressure or flow rate. It is recognised
125 that the Pedersen model was developed for oil applications but it has been shown to provide a
126 conservative prediction for the hydraulic modelling of CO₂ streams in the absence of a CO₂ viscosity
127 model (Wetenhall et al., 2014). The flow equation selected for this analysis was the Beggs and Brill
128 correlation (Beggs and Brill, 1973) with the Moody friction factor (Moody, 1944) as defined in Brill
129 and Mukherjee (1999).

130

131 **2.2. Modelling the heat transfer from the fluid to the surrounding soil**

132 To calculate the rate of heat transfer from the fluid contained inside the pipeline to the surrounding
133 soil, the pipeline is first divided into segments. The maximum segment length was set to 0.05m, as it
134 was found that the results were not sensitive to smaller segmentation lengths. For each segment, a
135 heat transfer balance is performed using the First Law of Thermodynamics, *i.e.* the total amount of
136 energy entering the pipeline segment must equal the amount of energy leaving the segment plus the
137 energy transferred to or from the surroundings. The hydraulic modelling procedure couples the
138 change in fluid properties with the heat and work done to the fluid through the pipeline segment.

139

140 For steady state flow, the First Law of Thermodynamics for a pipeline segment may be written as
141 (Mohitpour et al., 2003):

$$\Delta \left\{ \left(H + \frac{1}{2} v_m^2 + gz \right) dm \right\} = \Sigma \delta Q - \delta W \quad (1)$$

142

143 where the first three terms on the left hand side of the equation represent the changes in enthalpy,
 144 kinetic and gravitational potential energy respectively; v_m is the mean velocity of the fluid being
 145 transported in the pipeline, g is the gravitational constant, z is elevation, δQ is the amount of heat
 146 energy transferred to or from the pipeline segment and δW is the work done to the fluid. For steady
 147 state heat transfer caused by a difference between two temperatures, in this case the fluid (T_f) and the
 148 surrounding soil (T_g), the total amount of heat transferred through a pipeline segment may be written
 149 in terms of a conduction shape factor, S , which is defined by:

$$Q = 2\pi k_g S \Delta T \quad (2)$$

150
 151 where k_g is the thermal conductivity of the soil, ΔT is the temperature difference between the fluid and
 152 soil, Q is the amount of heat energy transferred and S depends on the geometry of the system (some
 153 examples of S are listed in Kreith and Bohn (2001)).

154
 155 For a buried pipeline, a solution for the conduction shape factor with convective boundary conditions
 156 for the interfaces between the pipeline and fluid film and between the ground and ambient air is
 157 facilitated by the use of bipolar cylindrical coordinates: (α, τ, z) . If z is set to the pipeline burial depth
 158 measured to the centre of the pipeline, Z , and D_o is the outside diameter then the lines
 159 $\alpha = 0$ and $a = \alpha_o = \cosh^{-1} \frac{2Z}{D_o}$ of the pipeline represent the ground surface and outer pipeline wall
 160 respectively (which are where the convective boundary conditions are applied). A solution, which
 161 closely agrees to numerical solutions in the literature, can then be found (Ovuworie, 2010):

$$S = \frac{Bi_p a_{bur}}{\sqrt{\left(\cosh \alpha_o - Bi_p a_{bur} \alpha_o + \frac{Bi_p}{Bi_g}\right)^2 - \left(1 + \frac{Bi_p}{Bi_g}\right)^2}} \quad (3)$$

162
 163 where

$$\alpha_o = -\cosh^{-1} \frac{2Z}{D_o} \quad (4)$$

164

$$a_{bur} = 4 \frac{Z^2}{D_o^2} - 1 \quad (5)$$

165
 166 k_g is the thermal conductivity of the soil and Bi_p and Bi_g are the Biot numbers of the pipeline and
 167 ground given by:

$$Bi_p = \frac{U_{pipe} D_o}{2k_g} \quad (6)$$

168

$$Bi_g = \frac{h_a D_o}{2k_g} \quad (7)$$

169

170 Here, h_a is the heat transfer coefficient of the fluid film of ambient air at the ground surface and the
 171 overall heat transfer coefficient of the pipeline, U_{pipe} , is a combination of the heat transfer coefficients
 172 of the fluid film, h_{film} , and pipeline, h_{pipe} :

$$\frac{1}{U_{pipe}} = \frac{1}{h_{film}} + \frac{1}{h_{pipe}} \quad (8)$$

173

174 The heat transfer coefficients of the pipeline and the films of fluid between the pipeline and internal
 175 fluid and the ambient air and soil can be determined by considering the layers between the fluid and
 176 pipeline wall (convective) and radially outwards through the pipeline wall (conductive) separately.

177

178 **2.2.1. Heat transfer between the ambient air and surface of the soil**

179 Heat transfer from the surface of the soil to the film of ambient air at the surface is convective and the
 180 corresponding heat transfer coefficient may be split into a free convection component, h_{free} ,
 181 (capturing the density differences) and a forced convection component, h_{forced} , (capturing the effect
 182 of the wind):

$$h_a = h_{forced} + h_{free} \quad (9)$$

183

184 As the wind speed is below 0.5m/s close to the soil surface, the free convection component dominates
 185 so a limiting value of 4W/m²K was used for h_a (Schlumberger, 2010).

186

187 **2.2.2. Heat transfer between the fluid film and pipeline wall**

188 Heat transfer from the film of fluid at the surface of the pipeline to the inner pipeline wall is
 189 convective and the heat transfer coefficient for this layer may be expressed as:

$$h_{film} = \frac{k_f Nu}{D_i} \quad (10)$$

190 where k_f is the thermal conductivity of the fluid (calculated using SUPERTRAPP (NIST, 2007)), Nu
 191 is the Nusselt number and D_i is the pipeline inner diameter. For the flow conditions considered in this
 192 study, the flow regime is always seen to be turbulent (with Reynold's numbers of the order 10⁶), and
 193 therefore, for the Nusselt number, semi-empirical correlations of the Reynold's number and Prandtl
 194 number can be used (Kreith and Bohn, 2001):

$$Nu = 0.023 Re^{0.8} Pr^{0.33} \left\{ 1 + \left(\frac{D_i}{\delta L} \right) \right\} \quad (11)$$

195 where δL is the pipeline segment length and

$$R_e = \frac{\rho v_m D_i}{\mu} \quad (12)$$

196

$$Pr = \frac{\mu c_p}{k} \quad (13)$$

197 where μ is the viscosity and ρ is the density of the fluid.

198

199 **2.2.3. Heat transfer through the pipeline wall**

200 Heat is transferred through the pipeline by conduction. Applying Fourier's Law of Conduction to a
201 pipeline of homogenous material, it can be shown (Kreith and Bohn, 2001) that the heat transfer
202 coefficient through the pipeline wall (h_{pipe}) is given by:

$$\frac{1}{h_{pipe}} = \frac{D_o}{k_{pipe}} \ln \frac{D_o}{D_i} \quad (14)$$

203

204 where k_{pipe} is the thermal conductivity of the pipeline material. Equations (10) and (14) can then be
205 used in Equation (8) to give the heat transfer coefficient of the pipeline.

206

207 **2.2.4. Heat transfer from the fluid to the surrounding soil**

208 Once the heat transfer coefficient of the pipeline has been calculated, using the procedure in Section
209 2.2.3, Equations (2) and (3) can be combined to give the overall heat transferred to or from the fluid to
210 the surrounding soil. Equation (1) can then be used to perform an energy balance through the pipeline
211 segment and therefore determine the temperature of the CO₂ stream as part of the steady-state
212 hydraulic modelling process.

213

214 **3. PRELIMINARY STUDY**

215 A series of eight steady-state pipeline simulations was conducted as part of a preliminary study to
216 compare the model with previous results and investigate the influence of ground temperature, flow
217 rate, inlet temperature, burial depth (measured to the top of the pipeline), soil conductivity, inlet
218 pressure and CO₂ composition on the rate of temperature loss along the pipeline. Firstly a base case
219 study was established against which other scenarios could be compared. The specification of the
220 pipeline section used in the base case is presented in Table 1. The pipeline operating conditions are
221 assumed to be typical of the requirements of a pipeline designed to be part of an anchor project
222 supporting a CCS network. The flow rate was selected based on the White Rose project (AECOM,
223 2013). The operating pressure of 150 barg has been selected to ensure that the CO₂ remains in the
224 dense phase along the pipeline length. It has been assumed that the manufacture and construction

225 standards and practices for CO₂ pipelines will be similar to those used for natural gas pipelines and
226 therefore no insulation has been applied to the pipelines in the hydraulic model and the pipes have
227 been buried to a depth of 1.2m as measured from the top of the pipeline. This figure is considered to
228 be representative of the maximum depth of cover required for the construction of onshore pipelines in
229 the UK (PD8010-1, 2015). A roughness value of 0.0457mm has been used as the recommended value
230 for commercial steel pipelines (Mohitpour et al., 2003). The soil thermal conductivity is considered to
231 be constant along the length of the pipeline and has been taken to be 0.87W/mK, which is typical of a
232 moist sandy or clay type soil (McAllister, 2005). The ambient ground temperature has been set at 3°C
233 for the base case representing a winter scenario in the UK.

234

235 Having established this base case pipeline, seven cases were run to investigate the influence of ground
236 temperature, flow rate, inlet temperature, burial depth, soil conductivity, inlet pressure and CO₂
237 composition on the rate of temperature and pressure loss along the pipeline. The parameters that were
238 changed for each study from the base case are detailed in Table 2. Of particular note is the approach
239 taken to investigate the effect of composition. Previous work indicates that the influence of a
240 particular component in hydraulic analysis is highly influenced by the critical temperature and
241 pressure of the component or impurity relative to pure CO₂ (Race et al., 2012; Wetenhall et al., 2014).
242 In this respect, the two impurities that could be present from power plant capture plant, which have
243 the most divergent effects on hydraulic behaviour are sulphur dioxide (SO₂) and hydrogen (H₂). As a
244 result only these two components have been selected to represent a best and worst case.

245

246 **3.1. Preliminary study results**

247 For each case listed in Table 2, the pressure and temperature profiles along the 150km long pipeline
248 were determined. The results were then presented in terms of the pressure drop/km (barg/km) or
249 temperature drop/km (°C/km) and are shown in Figure 2 and Figure 3. The pressure and temperature
250 drops per km obtained in this study are in line with the current literature (Teh et al., 2015; Zhang et
251 al., 2006). In particular, (Teh et al., 2015) reports temperature drops of 0.04 to 0.05°C/km for
252 scenarios with similarity to Case 1.1 and (Zhang et al., 2006) reports pressure drops of 0.02 to
253 0.03bara/km for scenarios with similarity to Cases 1.1 and 3.1.

254

255 The maximum pressure drop observed was 0.05barg/km for Case 2.1, the scenario with a flow rate of
256 17MT/year and a ground temperature of 3°C. This is below pressure gradients quoted in the literature
257 for CO₂ pipelines which are around 0.2bar/km (Seevam et al., 2010; Vandeginste and Piessens, 2008).
258 It is therefore concluded that the pressure drop is not significantly affected by the input parameters.

259

260 In terms of temperature drop, the temperature of the fluid does not reach the temperature of the
261 surrounding soil along the length of the pipeline. A review of the temperature profiles in Figure 3

262 indicates that the inlet temperature, flow rate, burial depth and soil conductivity appear to have the
263 largest effects on temperature drop. Parameters which seem to have a lesser effect are ground
264 temperature and composition. However, it is recognised that these conclusions are drawn from a small
265 sample set and the interactions between parameters have not been studied in detail in this preliminary
266 analysis.

267 **4. SENSITIVITY ANALYSIS**

268 The next stage in the analysis was to conduct a sensitivity analysis using a Gaussian emulator
269 approach to identify which of the parameters investigated in the preliminary analysis had the strongest
270 influence on the temperature drop along the pipeline. The rationale behind this analysis was to
271 determine the operational parameters that could or should be controlled by a pipeline operator to
272 maximise temperature drop or whether the critical parameters were environmental in nature and
273 therefore more difficult or impossible to control.

274

275 **4.1. Gaussian emulator approach**

276 The technique that has been used for the sensitivity analysis is the Gaussian emulator approach using
277 the Gaussian Emulation Machine for Sensitivity Analysis (GEM-SA) software (GEM-SA, 2013)
278 which provides a statistical approximation with which it is possible to perform a sensitivity analysis.

279

280 In order to perform an accurate sensitivity analysis on a model with a number of interrelated inputs (in
281 this case ground temperature, flow rate, inlet temperature, burial depth, soil conductivity and inlet
282 pressure) and outputs (temperature drop), a large number of simulation model runs is required.

283 Running this number of models in PIPESIM is prohibitive in terms of time and computer resource
284 requirements. A Gaussian emulator takes a series of inputs and the corresponding series of outputs
285 from running the simulation model (PIPESIM) and creates an emulator of the simulator, from which
286 predictive runs can be made quickly and cheaply in terms of computer processing requirements. The
287 Gaussian emulator also gives a probability distribution to show how the simulator performs away
288 from the design points. If the emulator is able to approximate the results of the simulator accurately,
289 then a sensitivity analysis of the model using the emulator is an accurate approximation to the
290 sensitivity analysis of the simulator.

291

292 **4.2. Input for the Gaussian emulator**

293 The range of input data that was used for the Gaussian Emulator is shown in Table 3. The ranges were
294 selected such that operation is maintained at pressures above the bubble point curve in order to avoid
295 two-phase flow. For the sensitivity analysis, two simulations were conducted; one for the 914.4mm
296 Outside Diameter (OD) pipeline as specified in Table 1 and the other for a 610mm OD, 19.1mm wall
297 thickness pipeline. A 610mm OD pipeline was selected as this was the size of the pipeline proposed
298 for the White Rose project (AECOM, 2013), an example of a CO₂ pipeline designed to facilitate

299 development of a pipeline transportation network. The length of the 610mm OD pipeline and the pipe
300 roughness used in the simulation remained the same as detailed in Table 1.

301

302 A series of 200 datasets of training inputs for the Gaussian Emulator were generated using a maximin
303 Latin hypercube design¹. This ensures that a good sample set of inputs was selected with which to
304 build the emulator that covers the whole parameter set range. The range is shown in Table 3. Each of
305 the 200 datasets was run in PIPESIM to obtain the training outputs. The emulator was then built using
306 the GEM-SA approach (O'Hagan, 2004).

307

308 The emulator provides a statistical approximation indicating the likelihood that the predicted value is
309 the true output of the model, *i.e.* in this case the PIPESIM output. At the training points, the
310 uncertainty of not emulating the simulated value is zero; away from the training outputs the
311 distribution associated with the inputs gives a mean value for the output for a Gaussian process of
312 uncertainty around the mean, each of the six input variables having a normal distribution.

313

314 **4.3. Gaussian emulator results**

315 The Gaussian emulators provided a good predictor for the output from PIPESIM. The variance of
316 expected code outputs for the 914.4mm and 610mm OD pipelines were 0.003 and 0.005 respectively.
317 Furthermore, predictions of the emulators were made for five sets of randomly selected model inputs
318 and compared with the corresponding output from PIPESIM. Considering the difference between the
319 predictions and PIPESIM output both emulators had R^2 values of 1.00.

320

321 The results of the GEM-SA emulations for the 914.4mm and 610mm OD pipelines, using the input
322 parameter ranges given in Table 3 are plotted in Figure 4 and Figure 5 respectively. The magnitude of
323 the effect on the y-axis of each graph indicates the expected value of the temperature decrease of the
324 fluid obtained by averaging over all other inputs. Negative slopes on the graphs indicate that the effect
325 on heat transfer from the fluid to the soil decreases with increasing values of the input parameter, *i.e.*
326 the outlet temperature of the fluid will be higher with increasing values of the input parameter.
327 Similarly, a positive slope indicates that the effect on temperature decrease of the fluid increases with
328 increasing values of the input parameter, *i.e.* the outlet temperature of the fluid is lower with
329 increasing values of the input parameter. The plots also indicate the uncertainty in the emulated
330 results with the wider bands indicating more uncertain regions of the emulation. Full details of the
331 theory behind the sensitivity analysis are provided in Oakley and O'Hagan, 2004).

332

¹ Latin hypercube sampling is a statistical methodology for generating a sample of parameter values from a multi-dimensional distribution. The sampled variables are then randomly combined into plausible variable sets for one calculation of the output function (in this case outlet temperature).

333 It is noted that the effect of the input variables on the temperature loss show the same qualitative
334 behaviour between the two pipeline diameters. However, the magnitudes of the effects are slightly
335 different for each case as a change in pipeline diameter results in a change in the pressure gradient
336 along the pipeline and therefore the results cannot be compared quantitatively.

337

338 **4.3.1. Effect of input variables**

339 Figure 4a and Figure 5a illustrate the effect of varying inlet pressure on the outlet temperature. Over
340 the range of pressures investigated, it can be seen that changing the inlet pressure has very little effect
341 on the outlet temperature of the fluid, provided that the inlet pressure is high enough to avoid two
342 phase flow along the entire pipeline length. The input parameters were specifically selected for the
343 GEMS emulations to avoid two-phase flow.

344

345 The effect of varying inlet temperature of the fluid is shown in Figure 4b and Figure 5b and follows a
346 linear trend as you would expect from looking at Equation (2). With increasing inlet temperatures, the
347 heat transfer from the fluid to the soil is increased and therefore the outlet temperature of the fluid is
348 decreased. However, increasing the ground temperature has a linearly decreasing effect on heat
349 transfer from the fluid (Figure 4d and Figure 5d), *i.e.* increasing the ground temperature decreases the
350 effect on the outlet temperature of the fluid. The same trend is shown for increasing burial depth
351 (Figure 4e and Figure 5e) although the effect tends to an asymptotic value; indicating that above about
352 1m, the burial depth has little effect on the outlet temperature of the fluid.

353

354 Soil conductivity also shows asymptotic rather than a linear behaviour with higher soil conductivities
355 increasing the amount of heat transfer from the fluid and decreasing its outlet temperature (see Figure
356 4c and Figure 5c). However the effect is less marked above a soil conductivity of about 2.5W/mK.

357

358 As the graphs of Figure 4f and Figure 5f illustrate, flow rate has a significant effect on outlet
359 temperature. As the flow rate increases less heat is transferred from the fluid to the surrounding soil
360 and therefore the fluid outlet temperature is increased. Smaller flow rates will lead to lower fluid
361 velocities and thus increased heat transfer. However, it can be seen that the largest effects occur at
362 lower flow rates with asymptotic behaviour observed at higher flow rates. For example, for the
363 914.4mm OD pipeline, increasing the flow rate above 600kg/s will have a marginal effect on the
364 outlet temperature for the simulations conducted.

365

366 At high flow rates, the pressure drops more rapidly along the pipeline than at lower flow rates.
367 Consequently, the density of the fluid decreases along the pipeline and the velocity and the Reynolds
368 Number (R_e) increases. Most of the heat loss in turbulent flow is convective, as opposed to
369 conductive, and an increase in velocity causes an increase in turbulence and an increase in convective

370 heat transfer. At lower flow rates the density increases along the pipeline, the flow velocity decreases
371 and the convective heat transfer decreases.

372

373 However, the density of the fluid also affects the thermal conductivity of the fluid (Polyakov, 1991).
374 As the density increases in the pipeline operating region, the thermal conductivity of CO₂ increases
375 and the rate of heat transfer increases. These competing phenomena could account for the asymptotic
376 shape of the flow rate curve in Figure 4f and Figure 5f.

377

378 **4.3.2. Sensitivity Analysis Results**

379 As well as allowing the effect of each variable to be considered in turn (as demonstrated in Figure 4
380 and Figure 5), the GEM-SA analysis also allows the relative sensitivity of each variable and the
381 interaction between variables to be studied. Table 4 shows the total effect of each input and the
382 contribution to the total variance of each input (*i.e.* the scatter about the mean) for the range of
383 variables considered in Table 3. From this table it can be seen that inlet temperature and flow rate
384 (shaded in Table 4) have a much larger effect on outlet temperature than inlet pressure, ground
385 temperature, soil conductivity and burial depth. It is highlighted that the effect of flow rate is higher
386 for the larger diameter pipeline and the effect of inlet temperature is greater for the smaller diameter
387 pipeline.

388

389 The interaction effects between each pair of variables for the two diameters of pipeline are displayed
390 in Table 5 in terms of their contribution to the total variance. This analysis indicates that, for the range
391 of input values considered, the interaction between inlet temperature and flow rate has the greatest
392 effect for both of the pipelines considered. No higher orders were considered as the main and joint
393 effects account for 98% of the total variance.

394

395 **5. CONCLUSIONS**

396 As a result of the analysis conducted, it has been shown that the inlet temperature and flow rate have
397 the largest effect on temperature gradient for the two diameters of pipeline considered in this study.

398

399 The heat loss from the pipeline is dominated by the density of the CO₂ which in turn is affected by the
400 pressure and temperature drop along the pipeline. As a result, the relationship between outlet
401 temperature and flow rate has been shown to be highly non-linear.

402

403 In natural gas pipelines the internal fluid rapidly reaches ambient temperature (Deaton, 1941).
404 However, as shown in this study and in the literature, in dense or supercritical phase CO₂ pipelines
405 the rate of heat transfer can be slow. This can lead to potential problems, for instance, if the fluid is
406 'shut in' the pipeline for a period of time, then, since the fluid temperature has remained high, there

407 will be a quantity of heat energy transferred to the surroundings and the temperature of the
408 surrounding soil will be increased. The slow rate of heat loss also affects CO₂ pipeline transportation
409 performance as the CO₂ streams have higher density at lower temperatures.

410

411 Although environmental factors, such as ground temperature and soil conductivity, have a marginal
412 effect on temperature loss, this effect is weaker than the parameters which are controlled by the
413 pipeline design such as inlet temperature and flow rate. It can therefore be concluded that the
414 temperature loss along a pipeline is predominantly controlled by the design of the pipeline which can
415 in turn be dictated by the capture plant's design and operation. Consequently, the operating
416 parameters need to be selected very carefully, especially the flow rate, to control the temperature loss
417 along the pipeline. In future work it would be useful to explore the effect that greater cooling at the
418 capture plant has on the costs of transportation.

419

420 **6. ACKNOWLEDGEMENTS**

421 This work has been conducted under the auspices of the National Grid COOLTRANS research
422 programme (CO₂ Liquid pipeline TRANSPORTATION) project and the authors gratefully acknowledge
423 the financial support of National Grid. The authors would also like to thank Schlumberger for the
424 donation of the PIPESIM software through the Schlumberger University Donation scheme.

425

426 **7. REFERENCES**

- 427 AECOM, 2013. Yorkshire and Humber Cross Country Pipeline - White Rose preferred route corridor
428 report, www.ccs-humber.co.uk/Assets/downloads/whiterose_report.pdf: Accessed 08.02.17.
- 429 Becker, B.R., Misra, A., Fricke, B.A., 1992. Development of correlations for soil thermal
430 conductivity. *Int. Commun. Heat Mass Transf.* 19, 59-68.
- 431 Beggs, H.D., Brill, J.R., 1973. Study of two-phase flow in inclined pipes. *Journal of Petroleum*
432 *Technology* 25, 607.
- 433 Brill, J.P., Mukherjee, H., 1999. *Multiphase flow in wells*. Society of Petroleum Engineers,
434 Richardson, Texas.
- 435 Capture Power, 2016. K33: Pipeline Infrastructure and Design Confirming the Engineering Design
436 Rationale.
437 [https://www.gov.uk/government/uploads/system/uploads/attachment_data/file/532023/K33_Pipe](https://www.gov.uk/government/uploads/system/uploads/attachment_data/file/532023/K33_Pipeline_infrastructure_and_design_confirming_the_engineering_design_rationale.pdf)
438 [line_infrastructure_and_design_confirming_the_engineering_design_rationale.pdf](https://www.gov.uk/government/uploads/system/uploads/attachment_data/file/532023/K33_Pipeline_infrastructure_and_design_confirming_the_engineering_design_rationale.pdf): Accessed
439 08.02.17.
- 440 Deaton, W.M., Frost, E.M., 1941. Temperatures of natural-gas pipe lines and seasonal variations of
441 underground temperatures U.S. Dept. of the Interior, Bureau of Mines.
- 442 Dongjie, Z., Zhe, W., Jining, S., Lili, Z., Zheng, L., 2012. Economic evaluation of CO₂ pipeline
443 transport in China. *Energy Conversion and Management* 55, 127-135.
- 444 Drescher, M., Wilhelmsen, Ø., Aursand, P., Aursand, E., De Koeijer, G., Held, R., 2013. Heat transfer
445 characteristics of a pipeline for CO₂ transport with water as surrounding substance, 11th
446 International Conference on Greenhouse Gas Control Technologies, GHGT 2012, Kyoto, pp.
447 3047-3056.

448 Dunn, G., Carlson, L., Fryer, G., Pockar, M., 2008. Effects of Heat From a Pipeline on Crop Growth -
449 Interim Results, Environment Concerns in Rights-of-Way Management 8th International
450 Symposium. Elsevier, pp. 637-643.

451 Farris, C., 1983. Unusual Design Factors for Supercritical CO₂ Pipelines. *Energy Progress* 3, 150-
452 158.

453 GEM-SA, 2013. Gaussian Emulation Machine for Sensitivity Analysis (GEM-SA) software. Centre
454 for Terrestrial Carbon Dynamics, <http://www.tonyohagan.co.uk/academic/GEM/>.

455 Infochem, 2011. Multiflash, Version 3.7 ed. Infochem Computer Services Ltd.

456 Kreith, F., Bohn, M.S., 2001. Principles of heat transfer, 6th edition ed. Brooks Cole.

457 Lake, J.A., Johnson, I., Cameron, D.D., 2016. Carbon Capture and Storage (CCS) pipeline operating
458 temperature effects on UK soils: The first empirical data. *International Journal of Greenhouse
459 Gas Control* 53, 11-17.

460 McAllister, E.W., 2005. Pipeline rules of thumb handbook 6th Edition ed. Elsevier, Oxford.

461 Mohitpour, M., Golshan, H., Murray, A., 2003. Pipeline Design and Construction: A Practical
462 Approach Third edition ed. ASME Press.

463 Moody, L.F., 1944. Friction factors for pipe flow. *Trans ASME* 66, 671.

464 Naeth, M.A., Chanasyk, D.S., McGill, W.B., Bailey, A.W., 1993. Soil temperature regime in mixed
465 prairie rangeland after pipeline construction and operation. *Can Agric Eng* 35, 89-95.

466 Neilsen, D., MacKenzie, A.F., Stewart, A., 1990. The effects of buried pipeline installation and
467 fertilizer treatments on corn productivity on three eastern Canadian soils. *Canadian Journal of
468 Soil Science* 70, 169-179.

469 NIST, 2007. Thermophysical properties of hydrocarbon mixtures database (SUPERTRAPP), National
470 Institute of Standards and Technology, Version 3.2 ed.

471 O'Hagan, A., 2004. Bayesian analysis of computer code outputs: a
472 tutorial, <http://www.tonyohagan.co.uk/academic/pdf/BACCO-tutorial.pdf>.

473 Oakley, J.E., O'Hagan, A., 2004. Probabilistic sensitivity analysis of complex models: A Bayesian
474 approach. *J. R. Stat. Soc. Ser. B Stat. Methodol.* 66, 751-769.

475 Ovuworie, C., 2010. Steady-state heat transfer models for fully and partially buried pipelines,
476 International Oil and Gas Conference and Exhibition in China 2010: Opportunities and
477 Challenges in a Volatile Environment, IOGCEC, Beijing, pp. 1355-1381.

478 PD8010-1, 2015. Code of practice for pipelines, Part 1: Steel pipelines on land. British Standards
479 Institute.

480 Pedersen, K.S., Fredenslund, A., Christensen, P.L., Thomassen, P., 1984. Viscosity of crude oils.
481 *Chemical Engineering Science* 39, 1011-1016.

482 Peng, D.Y., Robinson, D.B., 1976. A new two-constant equation of state. *Industrial and Engineering
483 Chemistry Fundamentals* 15, 59-64.

484 Polyakov, A.F., 1991. Heat Transfer under Supercritical Pressures, *Advances in Heat Transfer*, pp. 1-
485 53.

486 Race, J.M., Wetenhall, B., Seevam, P.N., Downie, M.J., 2012. Towards a CO₂ Pipeline Specification:
487 Defining Tolerance Limits for Impurities. *Journal of Pipeline Engineering*.

488 Schlumberger, 2010. PIPESIM, 2010.1 ed.

489 Seevam, P.N., Race, J.M., Downie, M.J., Barnett, J., Cooper, R., 2010. Capturing carbon dioxide: The
490 feasibility of re-using existing pipeline infrastructure to transport anthropogenic CO₂, 8th
491 International Pipeline Conference, IPC2010, Calgary, AB, pp. 129-142.

492 Teh, C., Barifcani, A., Pack, D., Tade, M.O., 2015. The importance of ground temperature to a liquid
493 carbon dioxide pipeline. *International Journal of Greenhouse Gas Control* 39, 463-469.

494 Vandeginste, V., Piessens, K., 2008. Pipeline design for a least-cost router application for CO₂
495 transport in the CO₂ sequestration cycle. *International Journal of Greenhouse Gas Control* 2,
496 571-581.

- 497 Wetenhall, B., Race, J.M., Downie, M.J., 2014. The Effect of CO₂ Purity on the Development of
498 Pipeline Networks for Carbon Capture and Storage Schemes. *International Journal of*
499 *Greenhouse Gas Control* 30, 197-211.
- 500 Zhang, Z.X., Wang, G.X., Massarotto, P., Rudolph, V., 2006. Optimization of pipeline transport for
501 CO₂ sequestration. *Energy Conversion and Management* 47, 702.
- 502

Pipeline parameters		Unit
Outside diameter (OD)	914.4	mm
Wall thickness	25.4	mm
Pipeline length	150	km
Pipe roughness	0.0457	mm
Operating conditions		
Inlet pressure	150	barg
Inlet temperature	40	°C
Flow rate (CO ₂)	12	Mt/year
Environmental conditions		
Ground temperature	3	°C
Composition of CO ₂	100% CO ₂	
Burial depth	1.2	m
Soil conductivity	0.87	W/mK
Elevation profile	Flat	

504

505

Table 1: Input parameters for base case pipeline

506

507

Scenario 1: Effect of ground temperature		Ground temperature (°C)
	Case 1.1	14
	Case 1.2	5
	Case 1.3	3
Scenario 2: Effect of flow rate		Flow rate (MT/yr)
	Case 2.1	17
	Case 2.2	5
Scenario 3: Effect of inlet temperature		Inlet temperature (°C)
	Case 3.1	50
	Case 3.2	30
	Case 3.3	20
Scenario 4: Effect of burial depth		Burial depth (m)
	Case 4.1	0
	Case 4.2	2
Scenario 5: Effect of soil conductivity		Soil conductivity (W/m.k)
	Case 5.1	0.15
	Case 5.2	2
	Case 5.3	4
Scenario 6: Effect of inlet pressure		Inlet pressure (barg)
	Case 6.1	120
	Case 6.2	100
Scenario 7: Effect of fluid composition		Composition (wt%)
	Case 7.1	CO ₂ + 5% H ₂
	Case 7.2	CO ₂ + 5% SO ₂

508

509

Table 2: Case studies used in the preliminary study

510

511

Parameter	Range for 914.4mm OD Pipe	Range for 610mm OD Pipe
Inlet pressure (barg)	120 - 200	130 - 200
Inlet temperature (°C)	20 - 50	20 - 50
Ground temperature (°C)	0 - 15	0 - 15
Flow rate (kg/s)	15 - 1100	15 - 400
Soil conductivity (W/m.K)	0.1 - 4	0.1 - 4
Burial depth (m)	0 - 2	0 - 2

512

513

Table 3: Input parameters for GEMS emulations

514

515

Input Variable	Variance (%)	Total Effect	Variance (%)	Total Effect
	914.4mm OD Pipeline		610mm OD Pipeline	
Inlet Pressure (x1)	0.06	0.24	0.05	0.22
Inlet Temperature (x2)	23.33	30.50	39.11	45.05
Ground Temperature (x3)	6.10	9.28	9.45	12.28
Flow Rate (x4)	50.63	59.54	30.42	37.29
Soil Conductivity (x5)	5.48	8.82	9.38	13.82
Burial Depth (x6)	2.83	5.80	1.64	4.24

516

517

Table 4: Sensitivity analysis results for the 914.4mm and 610mm diameter pipelines

518

519

Joint Effect	Variance (%)	Joint Effect	Variance (%)
914.4mm OD Pipeline		610mm OD Pipeline	
x1.x2	0.01	x1.x2	0.01
x1.x3	0.02	x1.x3	0.02
x1.x4	0.05	x1.x4	0.02
x1.x5	0.01	x1.x5	0.01
x1.x6	0.01	x1.x6	0.01
x2.x3	0.05	x2.x3	0.08
x2.x4	4.87	x2.x4	3.20
x2.x5	0.51	x2.x5	0.88
x2.x6	0.39	x2.x6	0.21
x3.x4	1.69	x3.x4	1.03
x3.x5	0.18	x3.x5	0.34
x3.x6	0.16	x3.x6	0.09
x4.x5	0.58	x4.x5	0.90
x4.x6	0.29	x4.x6	0.13
x5.x6	0.82	x5.x6	0.81

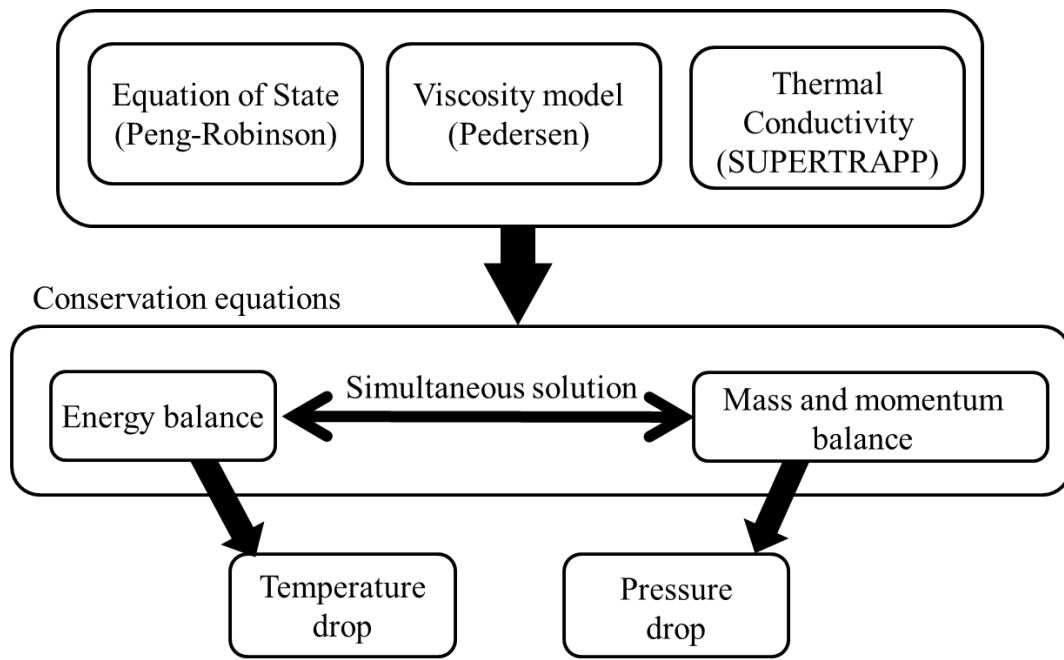
520

521

Table 5: Input parameter interaction effects for the 914.4mm and 610mm diameter pipelines (Table 4 shows the key for the variable names)

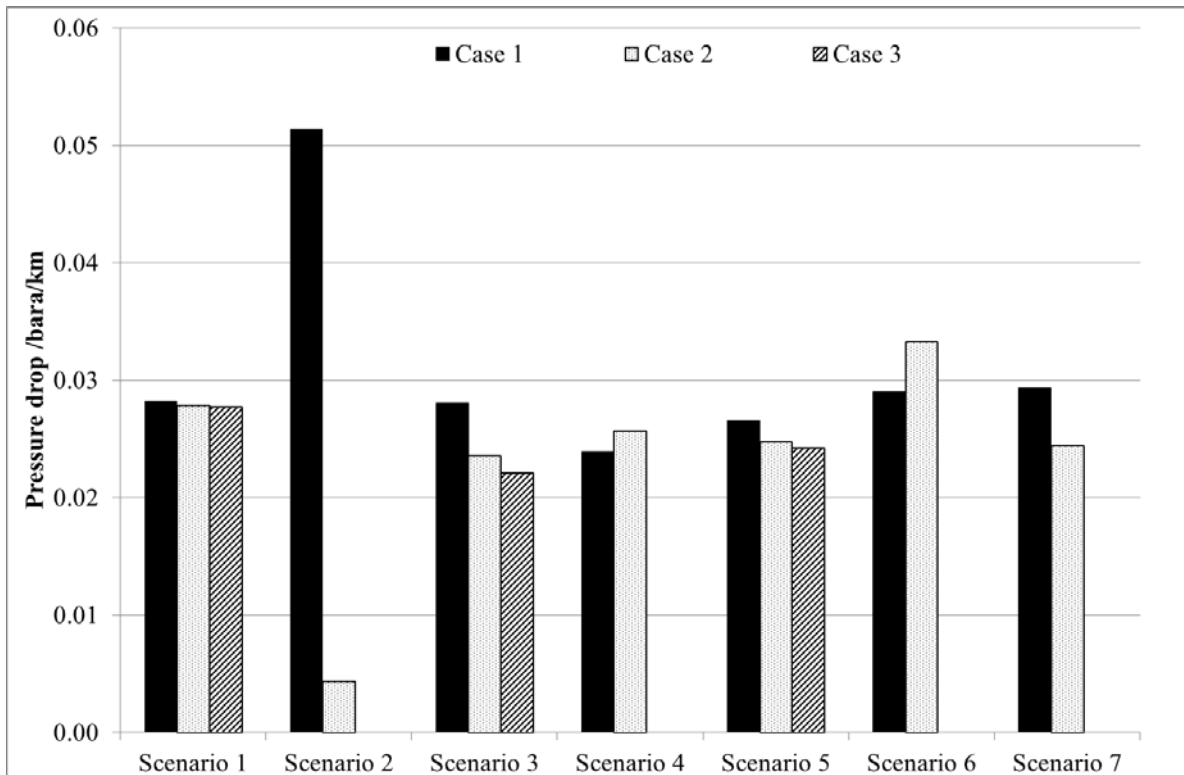
522

523



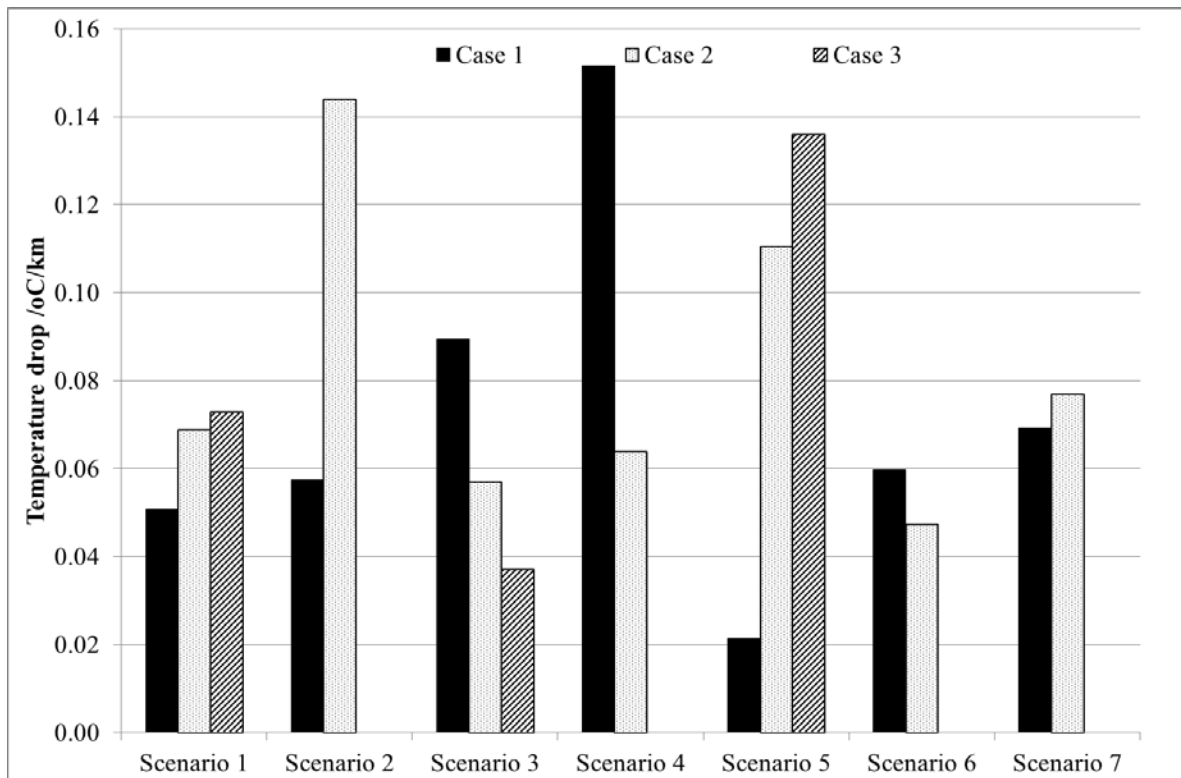
524
525
526
527

Figure 1: Flow diagram indicating the calculation methodology in the hydraulic analysis



528
529

Figure 2: Pressure drop per kilometre of pipeline for the case studies used in the preliminary study



530

531

532

533

Figure 3: Temperature drop per kilometre of pipeline for the case studies used in the preliminary study

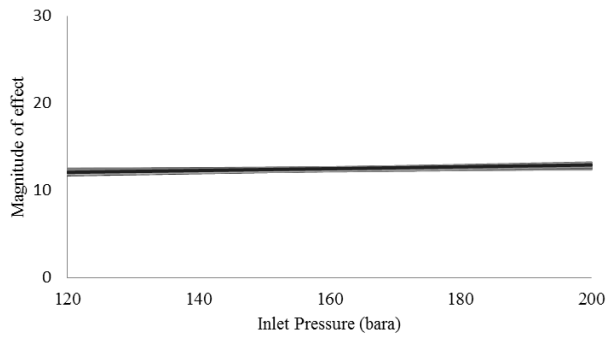


Figure 3a: Effect of Varying Inlet Pressure on Outlet Temperature

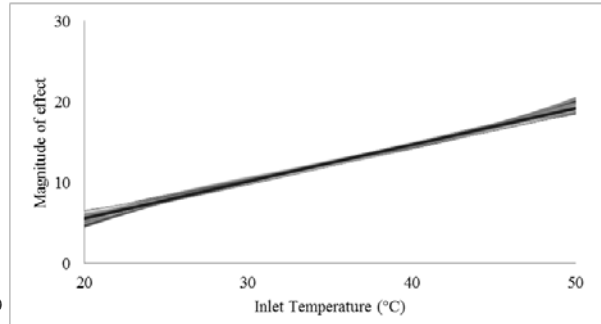


Figure 3b: Effect of Varying Inlet Temperature on Outlet Temperature

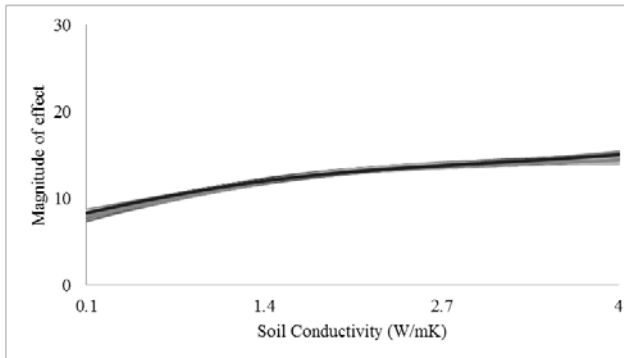


Figure 3c: Effect of Varying Soil Conductivity on Outlet Temperature

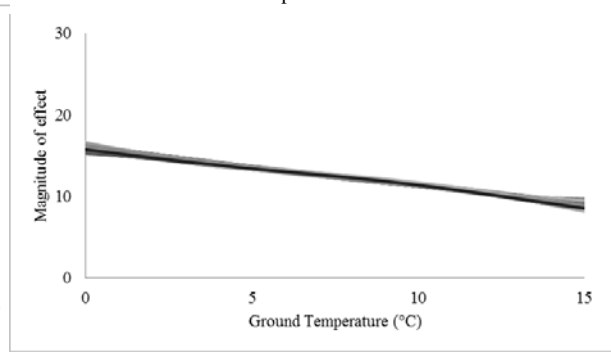


Figure 3d: Effect of Varying Ground Temperature on Outlet Temperature

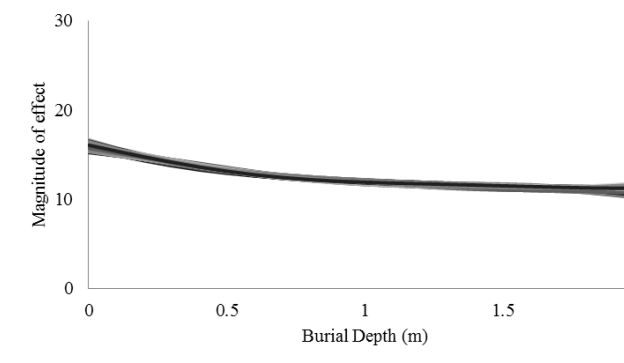


Figure 3e: Effect of Varying Burial Depth on Outlet Temperature

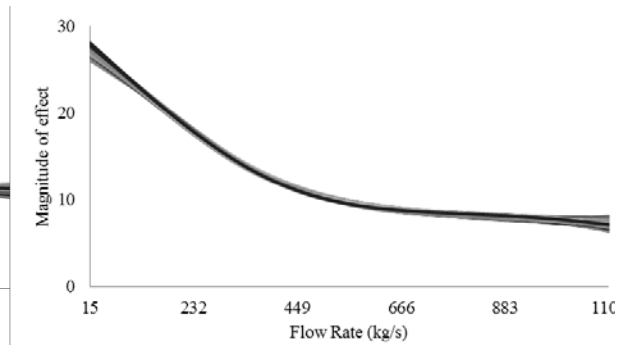
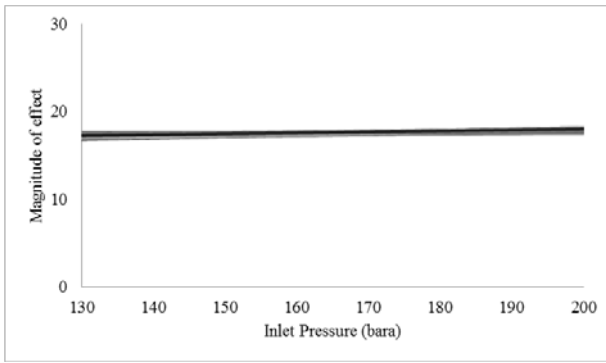


Figure 3f: Effect of Varying Flow Rate on Outlet Temperature

Figure 4: Effect of Study Parameters on Outlet Temperature for 914.4mm OD Pipeline

534
535
536
537



4a: Effect of Varying Inlet Pressure on Outlet Temperature

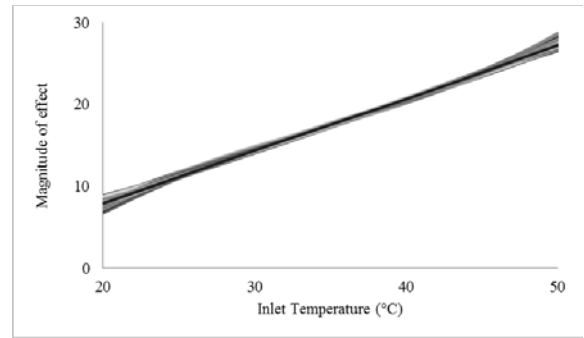


Figure 5b: Effect of Varying Inlet Temperature on Outlet Temperature

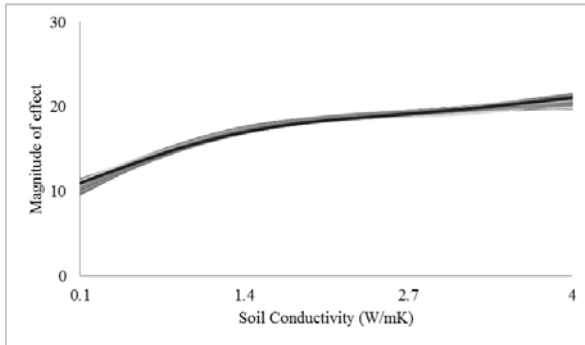


Figure 5c: Effect of Varying Soil Conductivity on Outlet Temperature

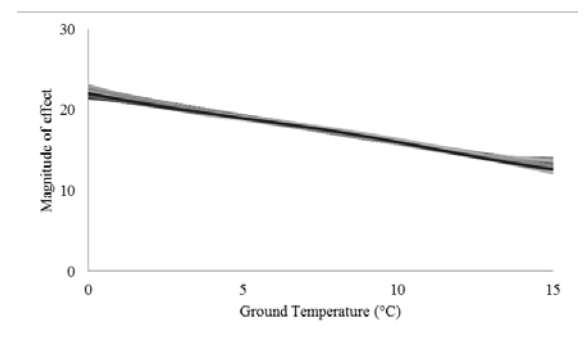


Figure 5d: Effect of Varying Ground Temperature on Outlet Temperature

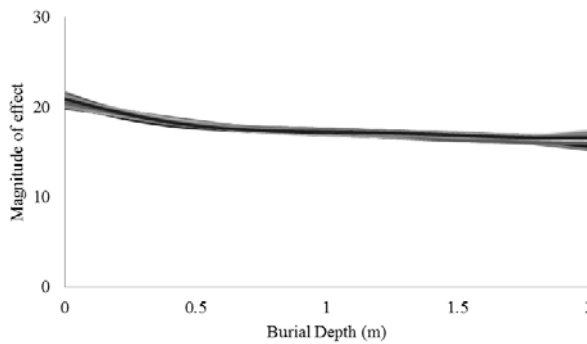


Figure 5e: Effect of Varying Burial Depth on Outlet Temperature

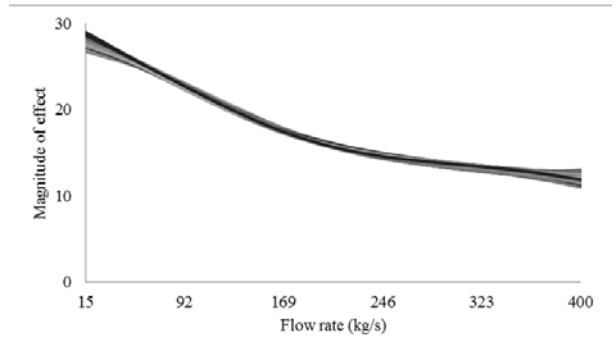


Figure 5f: Effect of Varying Flow Rate on Outlet Temperature

Figure 5: Effect of Study Parameters on Outlet Temperature for 610mm OD Pipeline

538

539

540